Nonlinear Analysis and Optimization of Diamond Cell Morphing Wings†

Terrence Johnson,[1] Mary Frecker,[2,*] Mostafa Abdalla[3]
Zafer Gurdal[3] and Doug Lindner[4]

[1]*Department of Aerospace Engineering, Penn State University, University Park, PA*

[2]*Department of Mechanical and Nuclear Engineering, Penn State University, University Park, PA*

[3]*Department of Aerospace Engineering, Delft University of Technology, The Netherlands*

[4]*Bradley Department of Electrical and Computer Engineering, Virginia Tech, Blacksburg, VA*

ABSTRACT: In this work, a two-stage design optimization procedure is developed to explore the effect of optimal actuator placement and position on energy efficiency in morphing wings. Diamond-shaped cells similar to NextGen's Batwing concept are used to examine this procedure. The finite element model considers elastic skin, actuator, and aerodynamic loads. Force displacement and efficiency studies are conducted using one and two unit cells, respectively. The model is then expanded to include multiple unit cells and actuators. A two-stage optimization process using a Genetic Algorithm and gradient-based optimization is also developed. The two-stage optimization is used to optimize actuator position and placement for different constraints and load cases. Results show that placement and position optimization produce small gains in energy efficiency; morphing using a soft isotropic skin is more efficient than stiff isotropic or anisotropic skins. In addition, the GA did not use all of the available actuators to maximize energy efficiency. The total actuator mass is also considered and is dependent on the maximum applied force per actuator and the number of actuators in the mechanism.

Key Words: optimization, morphing, aircraft, genetic algorithm, actuator placement.

INTRODUCTION

A morphing aircraft can be defined as an aircraft that changes its configuration to maximize its performance at different flight conditions. Aircraft morphing can occur by changing the configuration of different components of the aircraft, such as the fuselage, wing, engine, and tail (Jha and Kudva, 2004). An early example of wing shape change occurred when the Wright brothers used wing warping to control steering by bending the wing tips of the Wright B flyer. As aircraft flight evolved, and the speed of the aircraft increased, wing warping was replaced with an aileron system because the power requirements exceeded actuator capabilities and roll control devices based on wing warping had low loadability (Sanders et al., 2003; Campanile, 2006). Other examples of wing morphing are variable camber, variable span, variable incidence, and variable sweep wing (swing wing).

Current research initiatives are focused on large area changes to improve efficiency and control in different missions. The Defense Advanced Research Projects Agency (DARPA) has targeted three designs that demonstrate large area wing morphing by 150% or more: Lockheed Martin is exploring a rotating and folding wing; NextGen has developed a 'batwing' (Figure 1) concept with a large change in sweep and span; Raytheon is designing a wing that telescopes out of the fuselage. The Batwing concept is used as an example in this article to study effects of actuator placement and position on energy efficiency.

Some morphing wings use one large actuator that transmits force from a central location, which can add more material and weight to the aircraft. In addition, performance requirements may call for a large actuator that may not fit volumetrically inside the wing. As a result, optimally placed distributed actuators may be desired in order to decrease aircraft weight, decrease power requirements, and achieve morphing goals. Several examples of the optimal placement of actuators within structures and mechanisms appear in the literature. Li et al. (2001) optimized the size and location

*Author to whom correspondence should be addressed. E-mail: mxf36@psu.edu
Figures 1–4 and 6–17 appear in color online: http://jim.sagepub.com
†This paper was presented in part at the 2006 ASME-IMECE, paper number IMECE2006-14398.

1045-389X/09/07 0815–10 $10.00/0 DOI: 10.1177/1045389X08098098

Figure 1. *NextGen Aeronautics Batwing concept (Marks, 2003).*

of active material and the topology of the mechanical portion of flextensional actuators. A flextensional actuator can be defined as a piezoceramic (or a stack of piezoceramics) connected to a flexible mechanical structure that converts and amplifies the output displacement of the piezoceramic (Silva et al., 2000). Adali et al. (2000) used optimal actuator placement to minimize deflection of a laminated beam with unknown loading. The uncertainties associated with the unknown loading conditions lead to an anti-optimization problem, which is coupled to the optimal actuator placement problem via the design parameters and loading.

The previous examples describe the optimal placement of actuators using various optimization techniques. Examples of optimal actuator placement using the genetic algorithm (GA) are as follows: Simpson and Hansen (1996) used GA to optimally place actuators for noise reduction. The article shows how GA can be used to optimize actuator placement in situations where no direct analytical method is available for determining optimal actuator location configurations. Zhang et al. (2000) used a GA technique to optimally place piezoelectric actuators and sensors bonded with flexible smart structures. In this case, the location of the active elements is optimized to determine actuator and sensor placement and feedback gains. Han and Lee (1999) used GA to optimally place piezoelectric actuators and sensors on a composite plate for noise control. Sadri et al. (1999) used GA to optimally place piezoelectric actuators on isotropic plates to significantly improve vibration suppression. Bharti and Frecker (2003) developed an actuator placement method for compliant mechanisms using gradient-based optimization. The solutions with multiple actuators were shown to perform better than comparable single-actuator designs, but were complex and perhaps difficult to manufacture. Yan and Yam (2002) developed a methodology to determine the optimal number and locations of piezoelectric ceramic stack actuators for active vibration control of a space truss structure. The location optimization was conducted using GA. Ramrkahyani et al. (2005) and Bharti et al. (2005, 2006) used the parallel GA to optimize the location of truss member and cable actuators for morphing an aircraft structure. A ground structure approach was used and each member in the ground structure had four possibilities: (1) a truss member, (2) a cable that morphs the structure into a required shape, (3) a cable that is antagonistic and brings it back to the original shape, and (4) a void, i.e., the member does not exist in the structure.

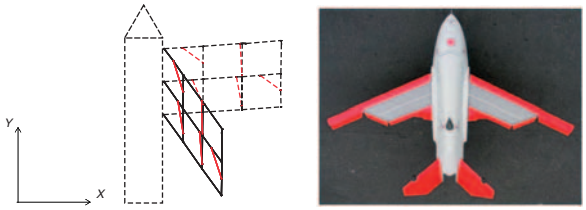

Figure 2. *NextGen Aeronautics Batwing concept and six unit cell scissor linkage model with distributed actuators – undeformed (solid) and deformed (dashed) shape (NextGen, 2008).*

This article explores the effects of optimal actuator placement and position on energy efficiency using a scissor mechanism similar to the NextGen Aeronautics Batwing design. The Batwing performs large area shape change by changing the wing sweep and span length. The aircraft uses a mechanism, powered by distributed hydraulic actuators, that moves with a scissor-like motion to morph the wing (Figure 2). The objective of this work is to investigate the arrangement of distributed actuation by optimizing actuator placement and position within each unit cell of the mechanism. The nonlinear finite element analysis approach is used to calculate the mechanism displacement and required actuator force. A two-stage optimization algorithm using a GA and MATLAB's FMINCON is used to conduct placement and position optimization. Several analyses are conducted to determine the effect of optimal actuator placement and position on energy efficiency and the need for placement and position optimization.

PROBLEM FORMULATION

Unit Cell

The scissor-linkage design is composed of diamond-shaped four-bar linkages called unit cells. The unit cells are joined to enable planar rotation of the wing in the clockwise and counterclockwise directions. A model of the scissors linkage with six unit cells is shown in Figure 3 where the X-axis is in the span-wise direction of the undeformed configuration. The green elements are the links of the mechanism, the red elements are the actuators, and the springs model the stiffness of the skin. The two-cell model on the right in Figure 3 illustrates the rigid connection between some of the links of the unit cells in the six-cell model. For example, elements 1 and 2 are constrained to have the same x, y, and θ displacements at node A. However, the rotational degree of freedom (dof) of element 5 is unconstrained at node A, i.e., element 5 can rotate relative to elements 1 and 2 at node A. Similarly, elements 3 and 4 are constrained to have the same x, y, and θ displacements, while element 6 can rotate relative to elements 2 and 4.

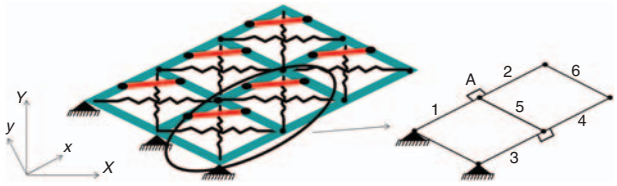

Figure 3. *Six unit cell scissor linkage model (undeformed) with axis system.*

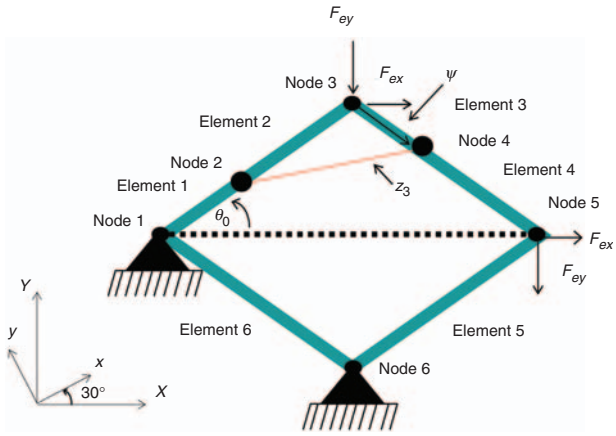

Figure 4. *Unit cell geometry.*

Table 1. Unit cell properties.

Material	Steel
Modulus (N/m^2)	1×10^6
Unit side length (m)	0.254
Actuator type	Pneumatic
Actuator extended length (m)	0.254

The finite element model of one unit cell is shown in Figure 4. The unit cell is oriented in the x–y coordinate system and it is shown in its initial position. The coordinate system is rotated 30° clockwise from the X-axis. The links (elements 1–6) of the unit cell are modeled as frame elements (3 dof per node) that are connected by pin joints. Geometric and material properties of the unit cell and actuator are shown in Table 1. Each unit cell has four sides and a side may be composed of one or more elements. The total length of each side of the unit cell is 0.254 m. When the unit cell is in its initial position (as shown in Figure 4), the actuator is in an open stoke position and the overall actuator length is 0.254 m.

In Figure 4, nodes 1 and 6 are connected to ground by pin joints. The loads F_{ey} and F_{ex}, located at nodes 3 and 5, model the aerodynamic loads on the wing and act in the negative y and positive x direction, respectively. They are assumed to be constant in this analysis. The actuator is connected to nodes 2 and 4. The position of the actuator within the unit cell is defined by a vector of magnitude ψ. Quantity ψ ranges between 0% and 100%. When ψ is 0%, node 4 is coincident with node 3, and when ψ is 100%, node 4 is coincident with node 5. Quantity z_3 represents the magnitude of the actuator length. Quantity θ_0 defines the initial half angle of the left corner of the unit cell. As the actuator is rotated within the unit cell, the magnitude of the actuator is fixed. The kinematics model was originally developed by Joo et al. (2006).

Efficiency

The goal of this work is to study the effect of optimal actuator placement and position on energy efficiency. In the literature, it is seen that energy efficiency is a common objective function in mechanism design (Hetrick and Kota, 1999; Prechtl and Hall, 1999; Prock et al., 2002; Johnson and Frecker, 2004; Abdalla et al., 2005; Joo et al., 2006). When energy efficiency is maximized, it indicates that output energy is maximized and input energy is minimized. A reduction in input energy may result in a reduction in the number of actuators in the wing, which would reduce the power required by the on board power supply, fuel consumption, and weight. Energy efficiency η is defined as the ratio of output energy to input energy (Equation (1)).

$$\eta = \frac{W_{\text{out}}}{W_{\text{in}}} \tag{1}$$

In this work, output energy, W_{out}, is defined as the work done by the mechanism against the aerodynamic loads (Equation (2)). The quantity X_{out} is the x component of displacement of the output point and it is directed opposite of F_{ex}. The quantity Y_{out} is the y component of displacement of the output and it is directed opposite of F_{ey}. The input work W_{in} is defined as the work done by an actuator on a unit cell (Equation (3)). The quantity F_{Act} represents the input force exerted on a unit cell by an actuator. The quantity Δ is the axial displacement of the actuator in the unit cell.

$$W_{\text{out}} = -\left(\sum F_{ex} X_{\text{out}} + \sum F_{ey} Y_{\text{out}}\right) \tag{2}$$

$$W_{\text{in}} = \sum F_{\text{Act}} \Delta \tag{3}$$

OPTIMIZATION

A two-stage optimization scheme is developed to maximize energy efficiency (Figure 5). In Stage 1, a GA is developed to conduct placement optimization of the actuators within the scissors mechanism. In Stage 2, MATLAB's FMINCON is used to conduct position optimization for each actuator within a unit cell. In both optimization schemes, the objective is to maximize energy efficiency. Actuator placement is defined as the existence of the actuators within the multiple unit cell model. Actuators can be placed in one or more

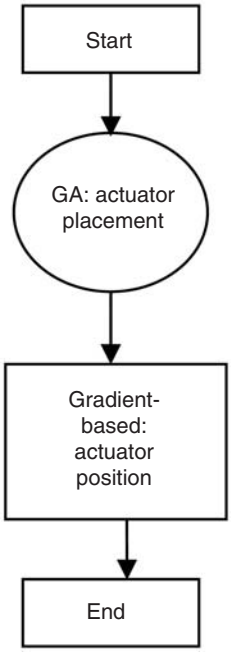

Figure 5. *Two-stage optimization procedure.*

unit cells in the six unit cell model. Actuator position is defined as the orientation of an actuator within a single unit cell.

Stage 1: Placement Optimization

In Stage 1, the GA maximizes efficiency (η) by optimizing actuator placement, or existence within each cell (Equation (4)). The optimization is subject to constraints on the output displacement of the mechanism (Δy) and the number of actuators allowed in the mechanism (N_{actu}). The design variables in the optimization represent actuator existence within each cell, which can have a value of 0 or 1.

$$\begin{aligned} \max\ \eta &= \frac{-\left(\sum F_{ex} X_{\text{out}} + \sum F_{ey} Y_{\text{out}}\right)}{\sum F_{\text{Act}} \Delta} \\ \text{s.t.} & \\ Y_{\text{out}} &= \Delta y \\ N_{\text{act}} &\le N_{\text{actu}} \end{aligned} \tag{4}$$

To be more specific, the scissor mechanism is modeled initially as if there is one actuator in each cell. The design variable, actuator existence, determines which cell(s) require actuation to maximize efficiency. A value of 0 denotes that an actuator is not active and it does not apply a force on the scissor mechanism, and a value of 1 denotes that the actuator is active and it exerts a force on the mechanism.

The GA is ideal for the actuator placement optimization because of its ability to handle the discrete (0–1) problem. In the optimization, the GA finds the best (fittest) solution to a problem based on genetic reproduction processes and 'survival of the fittest' strategies. The reader may refer to Onwubolu and Babu (2004) for a detailed explanation of the GA. In this work, each new population is developed by crossover, mutation, and elitism. Crossover and mutation are governed by a crossover and mutation percentage, respectively, that tells GA the maximum percentage of bits that may be crossed over or mutated to create a new individual of the population. The crossover percentage is set at 50% and the mutation percentage is set at 40%.

Stage 2: Position Optimization

Once the actuator placement problem has been solved, MATLAB's FMINCON is used to maximize efficiency (η) by optimizing actuator position (Equation (5)). The optimization is subject to a constraint on the output displacement of the mechanism (Δy) and the position of an actuator within a unit cell (ψ_i).

$$\begin{aligned} \max\ \eta &= \frac{-\left(\sum F_{ex} X_{\text{out}} + \sum F_{ey} Y_{\text{out}}\right)}{\sum F_{\text{Act}} \Delta} \\ \text{s.t.} & \\ Y_{\text{out}} &= \Delta y \\ 0.1 &\le \psi_i \le 0.95 \end{aligned} \tag{5}$$

MATLAB's FMINCON is a gradient-based solver that can be used to solve a constrained minimization problem. The positions of the actuators with the unit cells are represented by continuous variables ψ_i.

NONLINEAR ANALYSIS

Because the unit cells act almost like a mechanism, the nodal displacements are large and nonlinear analysis is required. Nonlinear finite element analysis is used to calculate the nodal displacements of the scissor mechanism and the actuator force. Joo et al. (2006) previously considered a first-order (linear) elastic analysis of one, two, and three unit cells. The current article incorporates a second-order elastic analysis by taking into account the affect of finite deformations and displacements of the system in the equations of equilibrium. The nonlinear FEA used in this work follows the formulation derived by Crisfield (1991) for corotational elements and displacement control; the reader is referred to his work for a detailed explanation. The links of the scissor mechanism are modeled as corotational elements and the orientation of the actuator force at each increment is considered in the formulation.

In this work, the Newton–Raphson iterative technique is combined with an incremental technique in order to control the displacement of the output node (output) of

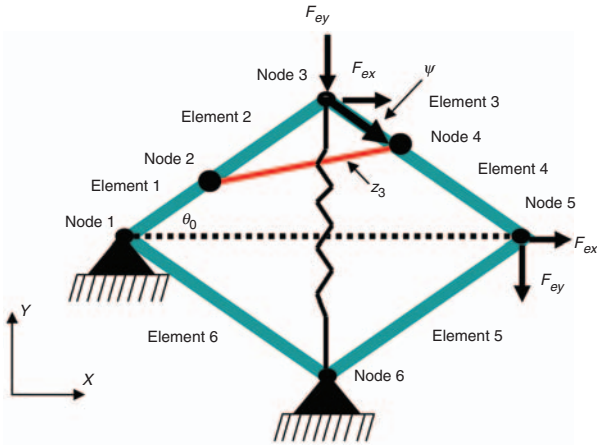

Figure 6. *Unit cell geometry w/spring.*

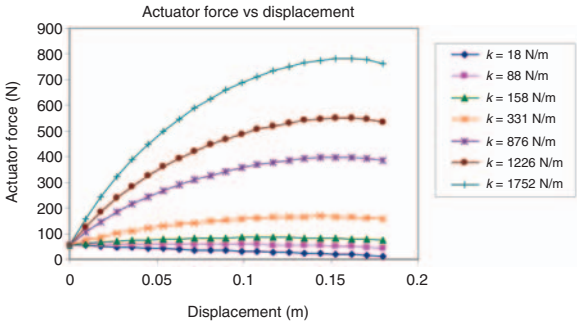

Figure 7. *Actuator force vs output displacement (Y_{out}) for one unit cell.*

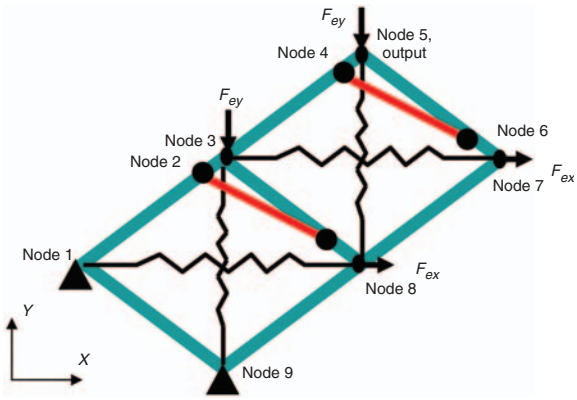

Figure 8. *Two unit cells.*

the scissor mechanism. In the six unit cell case, the maximum output displacement Δy is set to 533 mm in order to attain a rotation of 30°–90° counterclockwise of the entire mechanism about the positive z-axis (Figure 4).

RESULTS AND DISCUSSION

Several studies were conducted to show how optimal actuator placement and position affects energy efficiency for one-, two-, and six-cell scissor mechanisms. For one unit cell, a study is conducted to show the effects of actuator force on output displacement (Figure 6) using nonlinear analysis. In this case, the actuator is located at $\psi = 53\%$, the unit cell has one spring located in the y direction, and an aerodynamic load of $F_{ey} = 8$ N is located at output of the unit cell (node 3, Figure 6) directed in the negative y direction. The spring in the y direction is a simplified model of the skin stiffness. The spring is put into tension as the cell rotates counterclockwise. In this article, this scissor mechanism is actuated to rotate only in the counterclockwise direction; analysis and efficiency optimization for rotation in the clockwise direction is not considered.

The effect of varying spring stiffness can be observed in Figure 7. Because the external aerodynamic load is present, the initial actuator force is nonzero. Figure 7 shows that for spring stiffness (k) values above 158 N/m, the displacement of the output of the unit cell increases with an increase actuator force, and the force–displacement relationship is nonlinear. Since we are using displacement control to drive the nonlinear solver, the actuator force calculated using this technique represents the force required to maintain static equilibrium for a prescribed output displacement. Note that the actuator force required to maintain equilibrium at zero displacement is nonzero for all values of spring stiffness due to the presence of the external aerodynamic load. For values of k below 158 N/m, it can be observed that there is a negative stiffness effect, i.e., the applied actuator force decreases in order to maintain equilibrium. This is attributed to the orientation of the unit cell and the external load as the unit cell rotates counterclockwise.

In the two unit cell analysis, a study is conducted to show the effect of actuator position on energy efficiency (η). There are two actuators and they are assumed to have the same position in this study. Each cell contains two linear elastic springs that have a stiffness value of 851 N/m (Figure 8). There are aerodynamic loads in the x and y direction and each actuator in the mechanism has a constant force magnitude of $F_{\text{Act}} = 756$ N. Efficiency is calculated at actuator positions in the range of $\psi_i = 20$–80%. This range is selected because at positions 0–20% and 80–100%, 756 N of applied actuator force is not large enough to cause the mechanism to rotate out of its initial position and efficiency cannot be calculated in this region. At ψ equal to 0 and 100%, the actuator is collinear with the links of the unit cell, which is not a physically practical solution. The spring stiffness and actuator load values are based on experimental testing of a similar mechanism conducted at the Air Force Research Laboratory (Joo, 2006). Figure 9 shows a comparison of mechanism efficiency and actuator position for the two-cell case. The x-axis represents actuator position ψ.

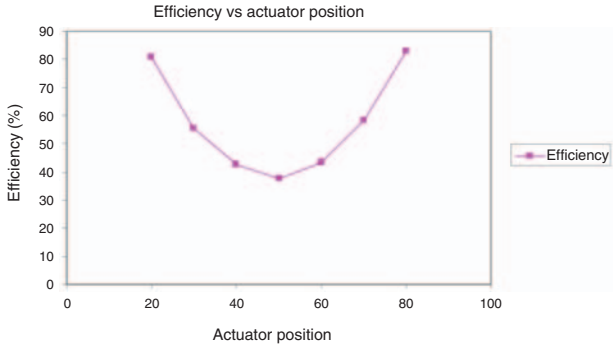

Figure 9. *Efficiency vs actuator position for two unit cells with constant actuator force.*

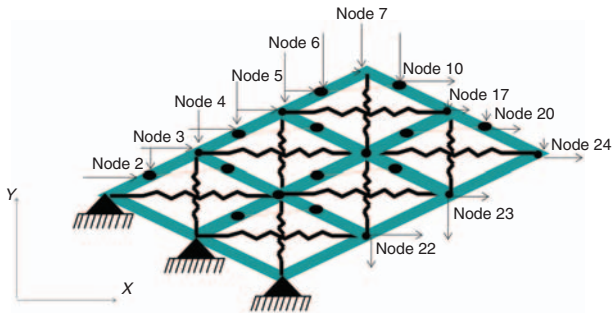

Figure 10. *Six-cell model with external loads.*

Figure 9 shows that maximum energy efficiency is attained when both actuators are positioned near the left or right corners of their respective unit cells. It was found that mechanisms with efficiency values between 50% and 90% have a lower output displacement than mechanisms with efficiency between 40% and 50%. This indicates that there is a trade-off between mechanism output displacement and efficiency. Figure 9 also shows a need to properly position the actuators within the scissor mechanism in order to maximize efficiency. As a result, the two-stage optimization algorithm was developed to conduct placement and position optimization on the actuators in many unit cells. The two-cell model is extended to six cells for this study.

In the six-cell model, each unit cell contains two springs directed in the x and y directions (Figure 10) representing the skin. The external aerodynamic loads are directed in the positive x and negative y directions. A detailed table of the magnitudes of the external aerodynamic loads per node is shown in Table A1 of the Appendix.[1] Eight different load cases were developed for this study (Table 2). Each load case is differentiated by its skin type and load level. The two orthogonal springs shown in each unit cell of Figure 10 represent average in-plane stiffness values of a continuous isotropic and orthotropic skin. Out-of-plane bending stiffness, Poisson's ratio effects, and in-plane shear deformation are not considered here

Table 2. Load cases.

Load case	Load level	Skin type
1	Low (5–22 N)	Isotropic, Soft k_x, $k_y = 122$ N/m
1a	Low (5–22 N)	Isotropic, Stiff k_x, $k_y = 851$ N/m
1b	Low (5–22 N)	Orthotropic, Soft x, Stiff y $k_x = 122$ N/m $k_y = 851$ N/m
1c	Low (5–22 N)	Orthotropic, Soft y, Stiff x $k_x = 851$ N/m $k_y = 122$ N/m
2	High (45–89 N)	Isotropic, Soft k_x, $k_y = 122$ N/m
2a	High (45–89 N)	Isotropic, Stiff k_x, $k_y = 851$ N/m
2b	High (45–89 N)	Orthotropic, Soft x, Stiff y $k_x = 122$ N/m $k_y = 851$ N/m
2c	High (45–89 N)	Orthotropic, Soft y, Stiff x $k_s = 851$ N/m $k_y = 122$ N/m

in modeling the skin. In addition, the compatibility of skin deformation with the substructure is neglected and these effects may contribute significantly to in-plane stiffness. Overall, four unique skin types and two unique load levels were considered.

The two-stage optimization process was conducted using an Intel Pentium 4 CPU 3.20 GHz, 1 GB of RAM. For the six-cell problem, one optimization run of the two-stage process requires ~20 min to find a solution. Several optimization runs, each with a different uniform starting point, were performed for each load case. In each run, a limit was put on the number of actuators that could appear in the final solution ($N_{\text{actu}} = 6, 5, 4, 3, 2, 1$). In all, 20 runs were performed per load case.

The effect of the number of actuators allowed in the two-stage optimization on energy efficiency is shown in Figure 11. In this study, the GA has a uniform starting point of $\psi_i = 0.5$ for each actuator position and the optimization results are restricted to have $N_{\text{actu}} = 5, 4, 3, 2$, or 1 actuators in the scissor mechanism. The results for load case 1b are pictured in Figure 11, where the red lines indicate the actuators in their optimized positions. In these cases, the output displacement was prescribed while the magnitude of input force provided by the actuator was unlimited. It can be observed that limiting the number of actuators does not greatly affect the overall energy efficiency. It can also be observed that the actuator positions tend toward one of the limits in each case.

Results of a study on the effect of the stiffness of the skin are shown in Figures 12 and 13. In this study, the optimizer is constrained to use only one actuator out of 6 (i.e., $N_{\text{actu}} = 1$) to maximize energy efficiency using

[1]The applied load distribution is based on data obtained from NextGen Aeronautics.

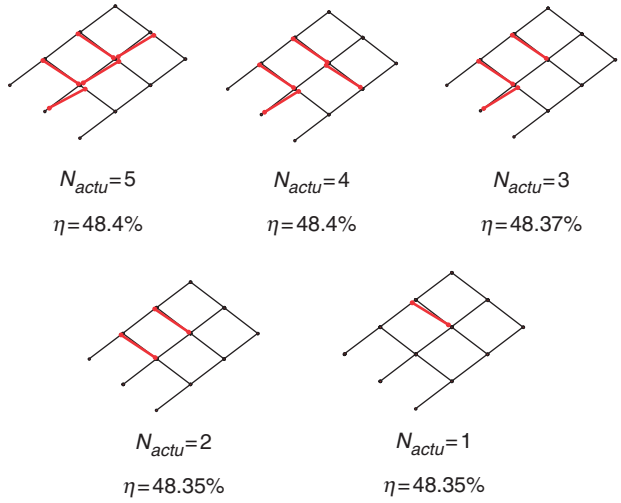

Figure 11. *Optimization results for load case 1b.*

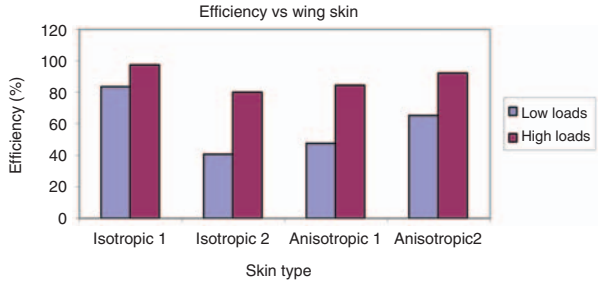

Figure 12. *Efficiency vs wing skin.*

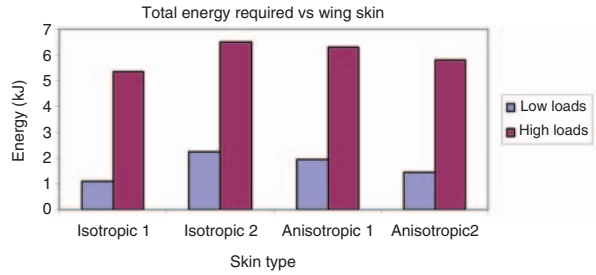

Figure 13. *Total energy required (input energy) vs skin stiffness.*

placement and position optimization. Results show that morphing under high loads (as defined in Table 2) is more efficient than morphing at low loads regardless of the skin stiffness. Efficient morphing under high loads is a consequence of having unlimited force input capability to achieve the displacement constraint. If a limit is placed on the actuator force, the mechanism may rotate, but the output displacement constraint may not be satisfied. It was also found that morphing under high loads requires more input energy than morphing under low loads (Figure 13). In this study, the most efficient design is one with soft isotropic skin under high or low air loads.

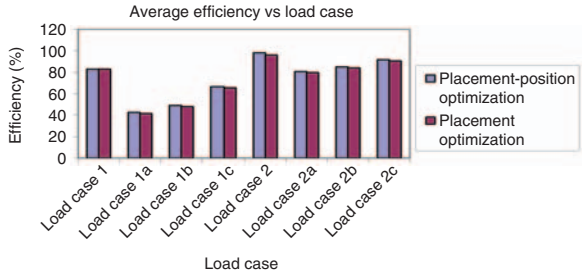

Figure 14. *Average efficiency vs load case.*

Figure 14 shows the average efficiency values per load case for placement optimization alone and placement followed by position optimization. The efficiency values from placement optimization were averaged over skin stiffness and compared to the average placement-position optimized solutions. The positions of the actuators at the starting point of position optimization were identical to the position of the actuators using the placement-only optimization. In both cases, the GA has a uniform starting point of $\psi_i = 0.5$ for each actuator position.

The results in Figure 14 show that in all load cases, a 2% gain at most, in average energy efficiency is achieved by conducting position optimization after placement optimization. As a result, it is concluded that the coupled placement-position optimization of the actuators may not be needed to the maximize energy efficiency of the scissor mechanism for this problem. It may be sufficient to simply optimize the actuator placement. It was also found that the optimizer generally positions the actuators in the 10 or 95% positions to maximize efficiency, which is similar to the results of two-cell study. Also, the placement optimization does not always use the total number of actuators available to maximize energy efficiency.

The previous results were obtained assuming that the actuator could provide an unlimited amount of force. The force required to meet the output displacement constraint varies, and as a result the mass of the actuator would also vary. Additional studies were conducted to estimate the actuator mass for various solutions. Marden and Allen (2002) showed that actuator force is related to motor mass for motors that use force production to accomplish steady translation motion of a load by the equation $\text{force} = 887 \times \text{mass}^{0.667}$. This relationship was used to estimate the total actuator mass based on the number of actuators in the mechanism and their maximum applied force (Figure 15). The results show that, in all load cases, actuator mass increases essentially monotonically with the required maximum actuator force.

Figure 16 shows the effect that the number of actuators in the mechanism has on the input energy needed to satisfy the output displacement constraint for load case 1a. A maximum actuator load constraint is set at 1090 N per actuator; the displacement

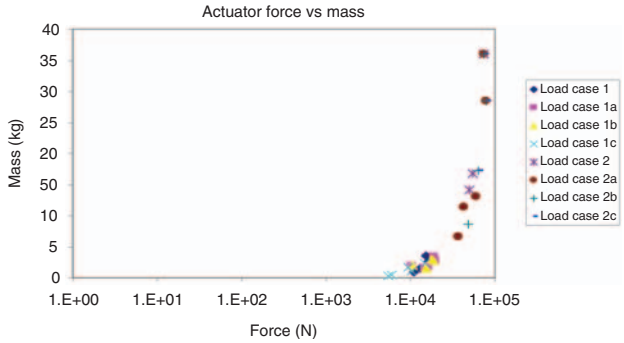

Figure 15. *Actuator force vs mass.*

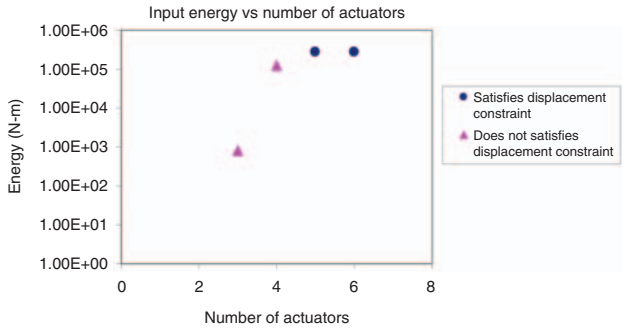

Figure 16. *Input energy vs number of actuators.*

constraint has not changed. Results show that for this problem at least five actuators are needed to satisfy the output displacement constraint. Once the output displacement constraint is satisfied, the input energy is then distributed among all available actuators.

Figure 17 shows the relationship between the total mass of actuators versus the number of actuators in the mechanism for the data in Figure 16. The load case and constraints are the same as those used in Figure 16. Results show that increasing the number of actuators in the mechanism does not necessarily result in an increase in total actuator mass. The mechanism with six actuators applies a maximum load of 3322 N lbs per actuator, while the solution with five actuators applies 3976 N per actuator. As a result, each individual actuator in the five-actuator case will be heavier than the actuators in the six-actuator case.

CONCLUSIONS

In this article, a methodology has been developed to study the effect of actuator placement and position on morphing wing energy efficiency. In this case, the methodology is used to study the effect of actuator placement and position using a scissor linkage mechanism similar to NextGen's Batwing concept. However, the methodology developed in this paper can also

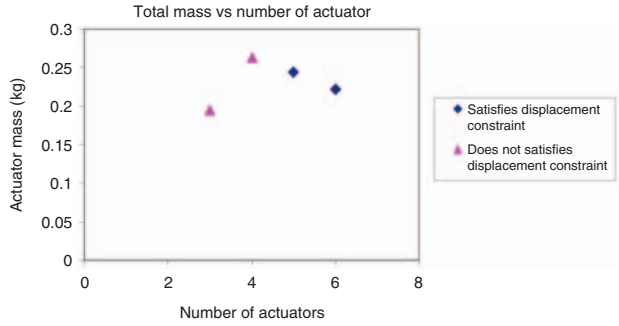

Figure 17. *Total mass vs number of actuators.*

be applied to morphing wings such as a telescoping or folding wing. The methodology includes: (1) defining a FEA model and analysis technique to solve the system, (2) defining an objective function for optimization, and (3) using a two-stage optimization procedure to determine both actuator placement and position within the system.

The results show that efficiency is dependent on aerodynamic loading and skin stiffness, and it is not greatly dependent on the number of actuators in the mechanism, or placement, or position optimization. Since efficiency is not greatly affected by the number of actuators within the mechanism, distributed actuation is a feasible solution for this mechanism. Results show that morphing under high loads is more efficient than morphing under low loads. This indicates that morphing may be possible while the aircraft undergoes different flight maneuvers. In addition, using the force–mass relationship, it was shown that total actuator mass increases with required maximum actuator force. This indicates that light-weight, high-energy density actuators are needed for wing morphing.

For future work, a study of energy efficiency and total work required using a more sophisticated model of the skin, e.g., a membrane-type element or a nonlinear material model, may be conducted. Additional objective functions such as actuator weight or axial stress in the unit cell should be considered. Finally, the 'unmorphing' problem should also be considered, as the aerodynamic loads will have a different effect in this case.

ACKNOWLEDGMENTS

The authors gratefully acknowledge the support of the Air Force Office of Scientific Research grant #FA9550-04-1-0124, and the Air Force Research Laboratory Air Vehicles Directorate Summer Research Program in collaboration with Dr Brian Sanders and Dr James Joo.

APPENDIX

Table A1. External aerodynamic loads.

Node number	Applied load (N)	Node number	Applied load (N)
2*x*	21.8	2*x*	88
2*y*	−9.3	2*y*	−57
3*x*	20.9	3*x*	85.8
3*y*	−13.8	3*y*	−67.2
4*x*	19.1	4*x*	81.4
4*y*	−17.8	4*y*	−75.6
5*x*	16.9	5*x*	75.6
5*y*	−20.5	5*y*	−84.9
6*x*	12.9	6*x*	65
6*y*	−22.2	6*y*	−89
7*x*	4.4	7*x*	44.5
7*y*	−17.8	7*y*	−81.4
10*x*	22.2	10*x*	89
10*y*	−20	10*y*	−83.2
17*x*	9.3	17*x*	57.4
17*y*	−4.9	17*y*	−45
20*x*	14.2	20*x*	69
20*y*	−5.3	20*y*	−46.7
22*x*	20.9	22*x*	85.9
22*y*	−13.8	22*y*	−67.2
23*x*	16.9	23*x*	75.6
23*y*	−17.8	23*y*	−82.3
24*x*	16	24*x*	61.8
24*y*	−5.3	24*y*	−46.7
(Low loads)		(High loads)	

REFERENCES

Abdalla, M.M., Frecker, M., Gurdal, Z., Johnson, T. and Linder, D.K. 2005. "Design of a Piezoelectric Actuator and Compliant Mechanism Combination for Maximum Energy Efficiency," *Smart Materials and Structures*, 14(6): 1421–1430.

Adali, S., Bruch Jr, J.C., Sadek, I.S. and Sloss, J.M. 2000. "Robust Shape Control of Beams with Load Uncertainties by Optimally Placed Piezo Actuators," *Structural and Multidisciplinary Optimization*, 19:274–281.

Bharti, S. and Frecker, F. 2003. "Compliant Mechanical Amplifier Design using Multiple Optimally Placed Actuators," In: *Proceedings of IMECE, ASME 2003 International Mechanical Engineering Congress and Exposition*, Washington DC.

Bharti, S., Frecker, M., Lesieutre, G. and Ramrakhyani, D. 2005. "Optimal Design of Tendon-actuated Morphing Structures: Nonlinear Analysis and Parallel Algorithm," In: *Proceedings of SPIE - The International Society for Optical Engineering, Smart Structures and Materials 2005 - Modeling, Signal Processing, and Control*, 5757:132–143.

Bharti, S., Frecker, M. and Lesieutre, G. 2006. "Optimal Structural Design of a Morphing Aircraft Wing using Parallel Non-dominated Sorting Genetic Algorithm II (NSGA II)," In: *Proceedings of SPIE - The International Society for Optical Engineering, Smart Structures and Materials 2006 - Modeling, Signal Processing, and Control*, 6166:616602.

Campanile, L.F. 2006. "Shape Adaptive Wings – The Unfulfilled Dream of Flight," In: Liebe, R. (ed.), *Flow Phenomena in Nature*, Siemens Power Generation, Mulheim, Germany, Vol. 2, pp. 400–419, WIT Press.

Crisfield, M.A. 1991. *Non-linear Finite Element Analysis of Solids and Structures*, Wiley, Chichester, New York.

Han, J. and Lee, I. 1999. "Optimal Placement of Piezoelectric Sensors and Actuators for Vibration Control of a Composite Plate using Genetic Algorithms," *Smart Material Structures*, 8:257–267.

Hetrick, J.A. and Kota, S. 1999. "Energy Formulation for Parametric Size and Shape Optimization of Compliant Mechanisms," *Journal of Mechanical Design, Transactions of the ASME*, 121(2):229–234.

Jha, A.K. and Kudva, J.N. 2004. "Morphing Aircraft Concepts, Classifications, and Challenges," In: *Proceedings of SPIE - The International Society for Optical Engineering, Smart Structures and Materials 2004 - Industrial and Commercial Applications of Smart Structures Technologies*, 5388:213–224.

Johnson, T. and Frecker, M. 2004. "Optimal Placement of Active Material Actuators using Genetic Algorithm," In: *Proceedings of SPIE - The International Society for Optical Engineering, Smart Structures and Materials 2004 - Modeling, Signal Processing, and Control*, 5388:221–231.

Joo, J.J., Sanders, B., Johnson, T. and Frecker, M.I. 2006. "Optimal Actuator Location within a Morphing-wing Scissor Mechanism Configuration," In: *Proceedings of SPIE - The International Society for Optical Engineering, Smart Structures and Materials 2006 - Modeling, Signal Processing, and Control*, Vol. 6166.

Li, Y., Xin, X., Kikuchi, N. and Saitou, K. 2001. "Optimal Shape and Location of Piezoelectric Materials for Topology Optimization of Flextensional Actuators," In: *Proceedings of the Genetic and Evolutionary Computation Conference*, San Francisco, CA.

Marden, J.H. and Allen, L.R. 2002. "Molecules, Muscles, and Machines: Universal Performance Characteristics of Motors," In: *Proceedings of the National Academy of Science*, 99:4161–4166.

Marks, P. 2003. "The next 100 years of flight – part two," NewScientist.com website, 17 December 2003. http://www.newscientist.com/article.ns?id = dn4484

NewScientist.com website. http://www.newscientist.com/article.ns?id = dn7552

NextGen Aeronautics. 2008. http://www.nextgenaero.com/index.html

Onwubolu, G.C. and Babu, B.V. 2004. *New Optimization Techniques in Engineering*, Springer, Berlin, New York.

Prechtl, E.F. and Hall, S.R. 1999. "Design of a High Efficiency, Large Stroke, Electromechanical Actuator," *Smart Material and Structures*, 8:13–30.

Prock, B.C., Weisshaar, T.A. and Crossley, W.A. 2002. "Morphing Airfoil Shape Change Optimization with Minimum Actuator Energy as an Objective," In: *9th AIAA/ISSMO Symposium on Multidisciplinary Analysis and Optimization*, AIAA:2002–5401.

Ramrkahyani, D.S., Lesieutre, G., Bharti, S. and Frecker, M. 2005. "Parallel Genetic Algorithm for Design of Morphing Cellular Truss Structures," In: *American Society of Mechanical Engineers, Aerospace Division (Publication), Proceedings of the ASME Aerospace Division*, 70:401–410.

Sadri, A.M., Wright, J.R. and Wynne, R.Y. 1999. "Modeling and Optimal Placement of Piezoelectric Actuators in Isotropic Plates using Genetic Algorithms," *Smart Material Structures*, 8:490–498.

Sanders, B., Eastep, F.E. and Forster, E. 2003. "Aerodynamic and Aeroelastic Characteristics of Wings with Conformal Control Surfaces for Morphing Aircraft," *Journal of Aircraft*, 40(1):94–99.

Silva, E., Nishiwaki, S. and Kikuchi, N. 2000. "Topology Optimization Design of Flextensional Actuators," *IEEE Transactions on Ultrasonics, Ferroelectrics, and Frequency Control*, 47(3):657–671.

Simpson, M. and Hansen, C. 1996. "Use of Genetic Algorithms for Optimizing Vibration Actuator Placement for Minimizing Sound Transmission into Enclosed Spaces,"

In: *Proceedings of SPIE Smart Structures and Materials Conference*, 2717:409–421.

Yan, Y.J. and Yam, L.H. 2002. "Optimal Design of Number and Locations of Actuators in Active Vibration Control of a Space Truss," *Smart Materials and Structures*, 11:496–503.

Zhang, H., Lennox, B., Goulding, P.R. and Leung A.Y.T. 2000. "A Float-encoded Genetic Algorithm Technique for Integrated Optimization of Piezoelectric Actuator and Sensor Placement and Feedback Gains," *Smart Materials and Structures*, 9(4):552–557.